Journal of Cellular Biochemistry 101:723–734 (2007)

Fat-Loaded HepG2 Spheroids Exhibit Enhanced Protection From Pro-Oxidant and Cytokine Induced Damage

Leonard H. Damelin,* Sam Coward, Michael Kirwan, Peter Collins, Clare Selden, and Humphrey J. F. Hodgson

UCL Institute of Hepatology, Hampstead Campus, Rowland Hill Street, London NW3 2PF, United Kingdom

Abstract The mechanisms by which steatosis renders hepatocytes susceptible to damage in non-alcoholic steatohepatitis (NASH) are unclear although fat accumulation is believed to increase hepatocyte susceptibility to inflammatory cytokines and oxidative stress. We therefore investigated the susceptibility of steatotic, hepatocyte-derived cells to TNFα and the pro-oxidant, t-butylhydroperoxide (TBH). HepG2 spheroids rendered steatotic by fat-loading with 0.15 mM oleic or palmitic acid for 48 h and treated with TNFα or TBH for 18 h exhibited surprisingly lower levels of cytotoxicity, and increased anti-oxidant activity (superoxide dismutase (SOD)) compared with non fat-loaded controls. The protective effect of steatosis was significantly reversed by the inhibition of AMP-activated kinase (AMPK) since spheroids transfected with a kinase-dead AMPKα2 subunit, exhibited a significant increase in TBH-induced cytotoxicity when fat-loaded. In conclusion, our findings suggest that fat-loaded hepatocyte-derived cells are surprisingly less susceptible to cytokine and pro-oxidant induced damage via an adaptive mechanism dependent, in part, on AMPK activity. J. Cell. Biochem. 101: 723–734, 2007.

Key words: NAFLD; NASH; oxidative stress; HepG2; spheroids; AMPK

Non-alcoholic fatty liver disease (NAFLD), a spectrum of liver damage ranging from steatosis to steatohepatitis (NASH) and cirrhosis is the most common liver disease in clinical practice [Farrell and Larter, 2006]. The mechanisms by which steatosis leads to hepatocyte damage and inflammation observed in NASH is not well understood although it has been correlated with increased inflammatory cytokine levels in the liver and periphery, elevated cytochrome P450 activity (specifically Cyp2E1 and 4A), impaired mitochondrial function, reduced cellular ATP levels, and oxidative damage [Machado and Cortez-Pinto, 2005; McCullough, 2006]. Based on this evidence, models have been proposed to explain the progression of NAFLD such as the widely accepted two-hit hypothesis put forward by Day and James [1998] which proposes that steatosis acts as a first hit rendering hepatocytes susceptible to damage by a variety of second hits. Whilst these secondary hits may vary (e.g., inflammatory cytokines such as TNFα, cytochrome P450 overexpression, direct fatty acid toxicity), it has been generally proposed that such secondary hits serve to increase the production of reactive oxygen species (ROS) in the steatotic hepatocyte resulting in cellular damage, necrosis and/or apoptosis and inflammation [Day, 2002; Nobili et al., 2005].

We have previously shown that culturing HepG2 cells in alginate beads creates cohesive cell colonies (spheroids) with markedly upregulated liver-specific detoxificatory and biosynthetic function, maximal at 8–10 days of culture [Khalil et al., 2001]. We therefore utilized this 3-D culture model to investigate the susceptibility of steatotic hepatocyte-derived cells to inflammatory cytokine, TNFα, and pro-oxidant challenge.

Grant sponsor: Liver Group Charity; Grant sponsor: Peter Samuel Memorial Fund.

*Correspondence to: Leonard H. Damelin, UCL Institute of Hepatology, Hampstead Campus, Rowland Hill Street, London, NW3 2PF, UK.
E-mail: l.damelin@medsch.ucl.ac.uk

Received 1 August 2006; Accepted 9 November 2006
DOI 10.1002/jcb.21229

Here we show that HepG2 spheroids become steatotic when exposed to oleic acid and when steatotic, spheroids are unexpectedly less susceptible to TNFα and to the pro-oxidant, t-butylhydroperoxide (TBH), than control spheroids. We conclude that a steatosis-induced adaptive response, which is partially dependent on AMP-activated kinase (AMPK) activation, renders cells less susceptible to oxidative stress.

MATERIALS AND METHODS

Reagents and Antibodies

Medium/cell culture supplements and fluorescent reagents were from Invitrogen (Paisley UK); labeled substrates were from Amersham GE (Buckinghamshire, UK) and PerkinElmer LAS (Milano, Italy). SAMS peptide was from Upstate (Dundee, UK); P81 phosphocellulose from Whatman (Middlesex, UK); rabbit anti-c-myc polyclonal antibody and donkey, anti-rabbit HRP-labeled antibody from Santa Cruz Technologies (Santa Cruz). Rabbit-anti AMPKα antibody from Cell Signaling Technology (Danvers). Other reagents were obtained from Sigma-Aldrich (Dorset, UK).

Cell Culture and Encapsulation

HepG2 cells from ECACC (Wiltshire, UK) were cultured in modified MEM-alpha (+4.5 g/L glucose) and encapsulated using an Inotech encapsulator as previously described [Damelin et al., 2004]. Briefly, cells were resuspended at a density of 0.5×10^6/ml in a mixture of one part 2% alginate (in 0.15 M saline) to one part culture medium. This combination was converted by the encapsulator to beads of an average diameter of 412 ± 17 μm which were gelled by being dropped into a gently stirred calcium chloride/sodium chloride solution (0.204 M $CaCl_2$/0.15 M NaCl pH 7.4) containing 0.01% pluronic acid. After washing in DMEM, beads were resuspended in culture medium and maintained at a ratio of 0.25 ml beads to 8 ml culture medium, 37°C and 5% CO_2 in air. Cells seeded within alginate beads proliferate forming multi-cellular colonies or spheroids after 5–7 days of culture: typically, one 450 μm alginate bead contains 20–25 spheroids and each spheroid consists of 8–20 HepG2 cells.

Transient Transfections

Plasmid pMEP 2E1 for the induced expression of cytochrome 2E1 isoform was produced by RT-PCR amplification of a 1,504 bp CYP 2E1 cDNA from human liver total RNA. The forward primer 5′-TCGGTACCGCC-ACCATGTCTGCCCTCGGAGTG-3′ and the reverse primer 5′-GCCTCGAGCTCATGAG-CGGGGAATGAC-3′, which incorporate KpnI and XhoI restriction sites, respectively, were used to facilitate direct cloning into the multiple cloning site of pMEP4 (Invitrogen), downstream of the inducible human metallothionein promoter. Sequencing of the construct through the coding region showed the CYP 2E1 sequence to be in agreement with the published sequence. Plasmid pAMPKα2 K45R expressing kinase-dead rat AMPK α2 subunit [Mu et al., 2001], was a generous gift from Dr M.J. Birnbaum (Howard Hughes Medical Institute, Philadelphia, PA). Transient transfections were performed with Lipofectamine 2000 (Invitrogen) at 4 μg plasmid DNA/1×10^6 cells.

Fat Loading of Spheroids

Spheroids maintained for 7 days were exposed for 48 h to medium with oleic or palmitic acid-BSA using fatty acid-BSA stock solution (100 mg/ml albumin in PBS, 2 moles fatty acid/mole albumin), final fatty acid concentration 0.15 or 0.3 mM. Fat-loading was assessed by transmission electron microscopy or by the fluorescent lipophilic dye, Nile Red [Greenspan et al., 1985].

Quantification of Gluconeogenesis

Spheroids were pulse-labeled for 3 h with U-^{14}C-glycerol in 2 ml αMEM. Medium aliquots were deproteinated (perchloric acid 4%), pelleted, neutralized with 5 M potassium hydroxide, and after spinning, 400 μl aliquots were applied to 0.3 g Amberlite MB-150 mixed-bed ion-exchange resin with 50 μl of 10 μCi/ml ^{3}H-glucose internal standard. Cleared supernatant, together with 200 μl wash eluant, was lyophilized, glucose separated by silica-TLC (using 1-butanol (104)/Ethanol (66)/H_2O (30)), detected using anisaldehyde, excised and ^{14}C and ^{3}H counted. Data are expressed as ratio of ^{14}C/^{3}H internal standard/total protein.

Lipid Biosynthesis

Spheroids were pulse-labeled with 2 μCi/ml 2-^{14}C-acetate in MEM-alpha supplemented with 25 mM HEPES (pH 7.4) for 2 h at 37°C. Lipids were extracted from spheroid pellets with 1 ml n-hexane/isopropanol (3:2 by volume)

for 1 h, acidified with 200 μl 3.5 M HCl and lyophilized. After washing (2×) with water, total labeled lipids were solubilized in 300 μl n-decane and quantified by scintillation counting [Scharnagl et al., 2001].

Fatty Acid Oxidation

Spheroids were fat-loaded for 48 h in medium with 1.5 μCi/ml 9,10-[^{3}H]Oleic acid. Fatty acid oxidation was assessed as in Shimabukuro et al. [1998].

Glucose Transport, ATP Quantification, Mitochondrial Membrane Potential, and Respiration

These were determined as previously described [Damelin et al., 2004].

Cytotoxicity Studies

Fat-loaded spheroids were exposed for 18 h to TNFα (2 or 0.2 ng/ml) with 1.6 μM actinomycin D or TBH (250–1,000 μM) and cytotoxicity assessed by (a) lactate dehydrogenase (LDH) release [CytoTox 96-Assay kit (Promega)]; (b) the cell-impermeable fluorescent dye, SYTOX Green, added to the medium with the toxicant (1 or 0.5 μM) [Jones and Singer, 2001]. After 18 h, spheroids were released from alginate and fluorescence quantified.

AMPK Activity Studies

AMPK activity was determined in spheroid lysates by the SAMS peptide assay [Salt et al., 1998].

TBARS Assay and NAD(P)H

Spheroids were removed from alginate and sonicated in 1.5 ml PBS. Lysate (100 μl) was incubated with 500 μl 20% trichloroacectic acid and 15 μl BHT (0.4 M in ethanol) for 10 min then 1 ml 0.67% TBA in water was added and samples heated to 100°C for 20 min. After centrifugation (5 min, 14,000*g*), fluorescence was read at 530 $nm_{excitation}$/580 $nm_{emission}$. The assay was optimized using MDA standards, values falling within the linear range, 10–0.3 μM MDA. A semi-quantitative measure of NAD(P)H was obtained from the absorbance of diluted lysate at 340 nm.

ROI Neutralizing Enzyme Activity and Reduced Glutathione Levels

Catalase was quantified in spheroid lysates using the method of Wu et al. [2003]. Superoxide dismutase (SOD) was quantified in spheroid lysates using an inverse luminescence assay, where the superoxide-dependent luminescence of lucigenin is quenched by SOD activity, according to Lenaerts et al. [2002]. Reduced glutathione was determined using monochlorobimane as in Sebastia et al. [2003].

Statistical Analyses

All assays were performed in triplicate (i.e., $n = 3$, each of the three samples being based on the analysis of 0.25 ml of alginate beads containing HepG2 spheroids). Unless otherwise stated in the legend, figures represent typical experiments where each investigation was repeated at least three times. Comparisons were by paired two-tailed Students *t*-test; results expressed as mean $\pm$ $SD_{(n-1)}$.

RESULTS

HepG2 Spheroids Exhibit Steatosis Upon Fat-Loading

HepG2 spheroids exposed to oleic acid for 48 h exhibited steatosis, proportional to fatty acid concentration as confirmed by Nile red staining and transmission electron microscopy (Fig. 1A–E).

Fat-Loading Decreases TNFα and Pro-Oxidant Induced Cytotoxicity

We investigated the effect of steatosis on the susceptibility of spheroids to TBH-induced oxidative stress and the pro-inflammatory cytokine, TNFα. Cytotoxicity was assessed using SYTOX Green which intercalates with the DNA of dead cells and those with damaged cytoplasmic membranes to form fluorescent complexes [Jones and Singer, 2001]. Surprisingly, spheroids rendered steatotic for 48 h, then exposed to TBH for 18 h exhibited lower SYTOX Green fluorescence (i.e., reduced cytoplasmic membrane damage) than non-steatotic controls (Fig. 2A). SYTOX Green fluorescence for fat-loaded spheroids exposed to TNFα with 1.6 μM actinomycin D was also significantly lower than for non-steatotic controls (Fig. 2B). To rule out interference to DNA binding by fat, we also assessed cytotoxicity by LDH release, confirming that fat-loaded spheroids exhibited a > twofold reduction in pro-oxidant induced cytotoxicity compared to untreated spheroids (Fig. 2C). This phenomenon was not peculiar to unsaturated fatty acid as both SYTOX Green

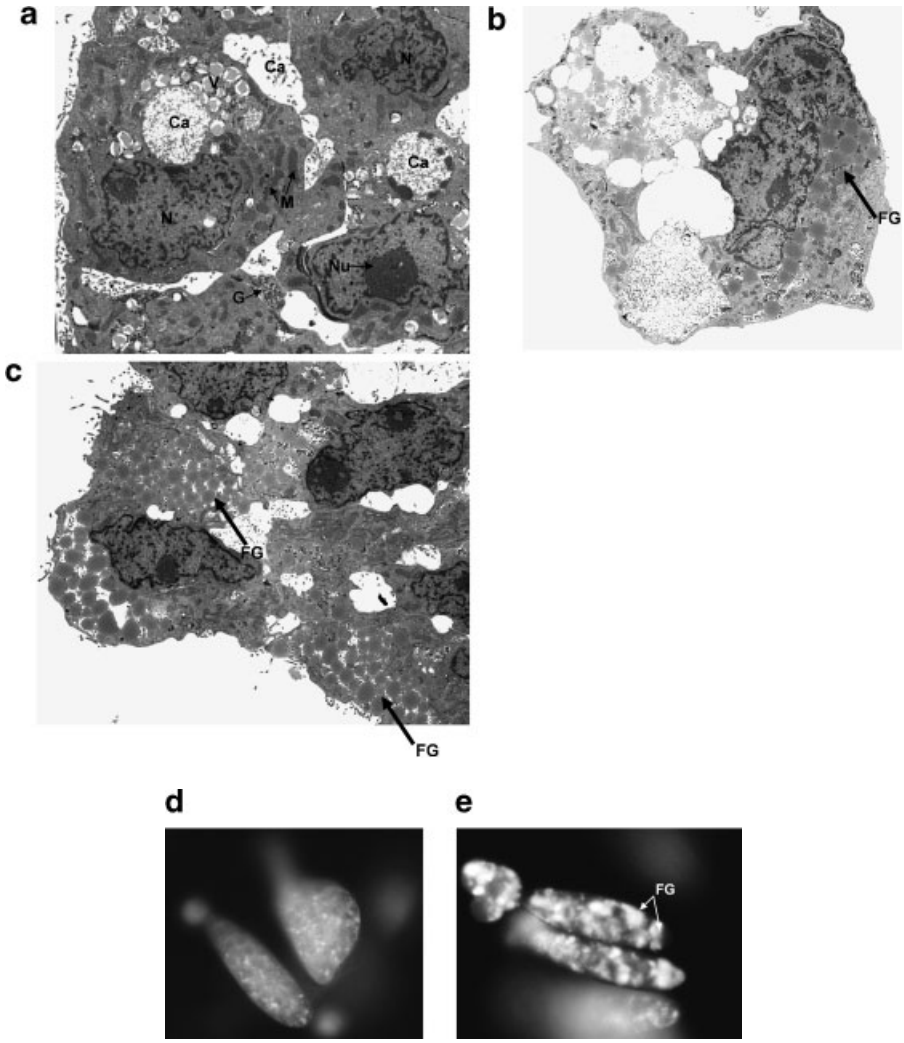

Fig. 1. Transmission electron micrographs (2,650 × magnification) of Day 7 HepG2 spheroids (multi-cellular cohesive colonies) exhibiting hepatocyte-like subcellular architecture with plentiful mitochondria (M), nuclei (N) with prominent nucleoli (Nu), vacuoles (V), glycogen (G), and canaliculi lined with microvilli (Ca). Spheroids exhibited steatosis upon exposure to (**b**) 0.15 and (**c**) 0.3 mM oleic acid for 48 h. Large arrows indicate spherical fat globules (FG) not apparent in **a** (non-fat loaded control). Spheroids were also exposed to 0 (**d**) or 0.15 mM (**e**) oleic acid for 48 h and stained with Nile Red (100 ng/ml), after which they were viewed by fluorescence microscopy (40 × magnification). Arrows indicate fluorescent fat globules (FG).

and LDH assays showed reduced cytotoxicity for spheroids fat-loaded with palmitic acid (Fig. 3A,B).

Since studies have associated increased expression of cytochrome P450 isoforms, specifically Cyp2E1, with the oxidative stress observed in NASH [Lieber, 2004] we investigated the possibility that intrinsically low cytochrome P450 expression by HepG2 cells [Rodriguez-Antona et al., 2002], was responsible for this protective effect. HepG2 transfectants containing a Cyp2E1 expression vector under the control of a metallothionein promoter were encapsulated in alginate, cultured for 7 days and fat-loaded with 0.15 mM oleic acid for 48 h. Twenty hours into fat-loading, copper sulfate was used to induce Cyp2E1 expression.

Cyp2E1 transfectants did not exhibit increased basal SYTOX green fluorescence when compared to empty vector control transfectants, but exhibited markedly increased (almost threefold) SYTOX Green fluorescence when exposed to 0.5 mM TBH for 18 h, indicating increased susceptibility to oxidative stress (Fig. 4). However, Cyp2E1 expression failed to ablate the protective effect of fat-loading.

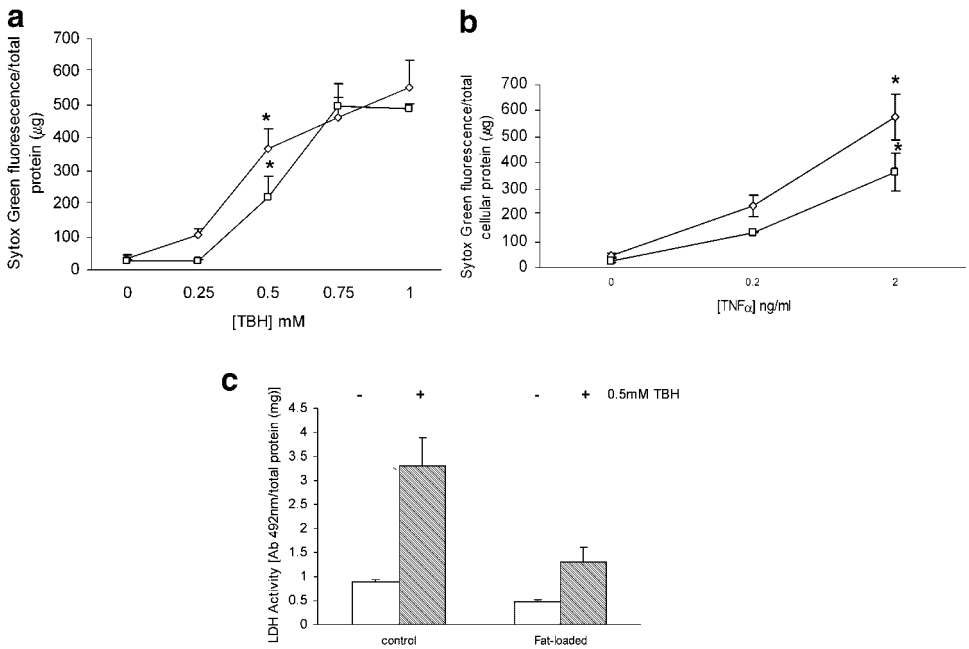

Fig. 2. Fat-loaded spheroids exhibit reduced cytotoxicty upon exposure to TBH and TNFα. **a**: Day 7 spheroids were untreated (diamond) or fat-loaded for 48 h with 0.15 mM oleic acid (square) and then exposed to varying doses of TBH for 18 h in the presence of SYTOX Green (1 μM). **b**: Untreated spheroids (diamond) and fat-loaded spheroids (square) as above, were also exposed to 0, 0.2, or 2 ng/ml TNFα in combination with 1.6 μM actinomycin D for 18 h in the presence of SYTOX Green. **c**: Untreated (Control) or Fat-loaded spheroids, as above were exposed to 0 (open bar) or 0.5 mM TBH for 18 h (shaded bar). LDH activity, proportional to tetrazolium reduction was quantified spectrophotometrically at 492 nm, and data are expressed as absorbance units per total protein (mg), $n = 3$, mean ± SD. a, b are an average of three experiments carried out in triplicate. Fat loading significantly decreased TBH and TNFα cytotoxicity for all three assays ($^*P < 0.05$).

Steatotic Spheroids Exhibit a Positive Redox Shift and Increased SOD Activity

A reduction in TBH-induced cytotoxicity by fat-loading suggested a potential upregulation of ROI neutralizing enzymes and/or increased NAD(P)H/reduced glutathione (GSH) levels in steatotic spheroids. Indeed, fat-loaded spheroids showed a significant (30%) increase in SOD activity compared to non-treated controls (Fig. 5A). No significant increase in catalase activity for fat-loaded spheroids was observed (Fig. 5A). However, intracellular GSH levels were halved by fat-loading and this coincided with a 16% reduction in intracellular NAD(P)H levels for fat-loaded spheroids (Fig. 5B). Interestingly, there was no significant increase in thiobarbiturate (TBA)-reactivity due to fat-loading (Fig. 5B). Thus, steatosis in this model induces a mild pro-oxidant state and triggers increased SOD activity in the absence of significant oxidative damage, this phenomenon appears to precondition against more severe oxidative stress.

Fat-Loading Induces a Phasic Increase in AMPK Activity

We investigated the effects of steatosis on spheroid metabolism and energetics. Fatty acid oxidation studies, where spheroids were fat-loaded with oleic acid spiked with tritiated oleic acid over 48 h and fatty acid oxidation assessed by the measurement of tritiated-H_2O production at 12 h intervals, indicated a progressive increase in fatty acid oxidation over time, proportional to fat uptake over 24–36 h (Fig. 6). ATP levels in fat-loaded spheroids were approximately 18% lower than non-steatotic controls (842 ± 113 and 700 ± 51 luminescence units/total protein (μg) for control and fat-loaded spheroids, respectively, $n = 3$, $P < 0.05$). There was a similar (19%) reduction in mitochondrial membrane potential (22 ± 1.64 and 18 ± 0.89 JC-1 aggregate/monomer fluorescence ratio/total protein (mg), $n = 3$, $P < 0.05$). However, lowered membrane-potential occurred without significant change in respiration demonstrated by unchanged O_2

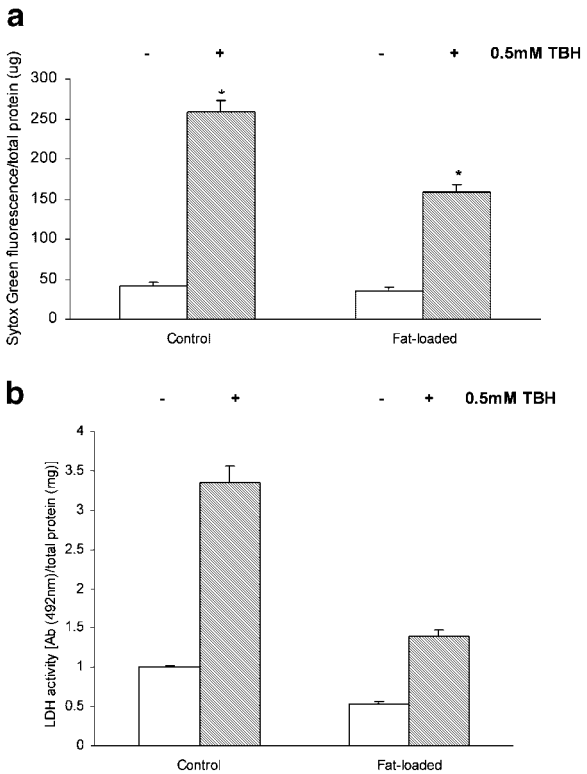

Fig. 3. Spheroids fat-loaded with palmitic acid exhibit reduced cytotoxicty upon exposure to TBH. Spheroids were untreated (Control), or Fat-loaded for 48 h with 0.15 mM palmitic acid and then exposed to 0 (open bar) or 0.5 mM TBH (shaded bar) for 18 h and (**a**) SYTOX Green fluorescence and (**b**) LDH activity was determined, n = 3, mean ± SD. a: Represents an average of three experiments carried out in triplicate. Fat-loading with palmitic acid significantly decreased TBH cytotoxicity (*$P < 0.05$).

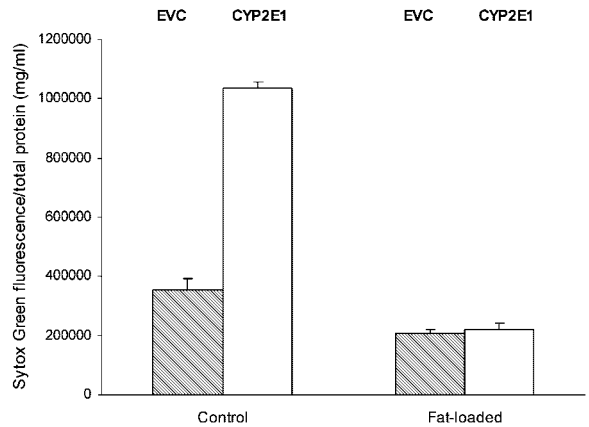

Fig. 4. Spheroids expressing CYP 2E1 exhibit increased susceptibility to oxidative stress. Day 7 spheroids from HepG2 cells transfected with an empty pMEP4 vector (shaded bar, EVC) or with a pMEP 2E1 vector expressing CYP2 E1 under the control of an inducible metallothionein promoter (open bar, CYP2E1) were untreated (Control) or fat-loaded with 0.15 mM oleic acid for 48 h (Fat-loaded). Twenty hours into fat-loading copper sulfate was used to induce CYP expression. Treated transfectants were then exposed to 0.5 mM TBH for 18 h with SYTOX green and fluorescence quantified, n = 3 mean ± SD.

consumption (data not shown), suggesting, as in a previous study [Kawaguchi et al., 2002], that reduced ATP levels were a likely consequence of increased fatty acid activation prior to oxidation rather than due to significant mitochondrial membrane uncoupling. More importantly, this previous study also showed that decreased ATP levels activate AMPK, leading to increased glucose transport and the down-regulation of

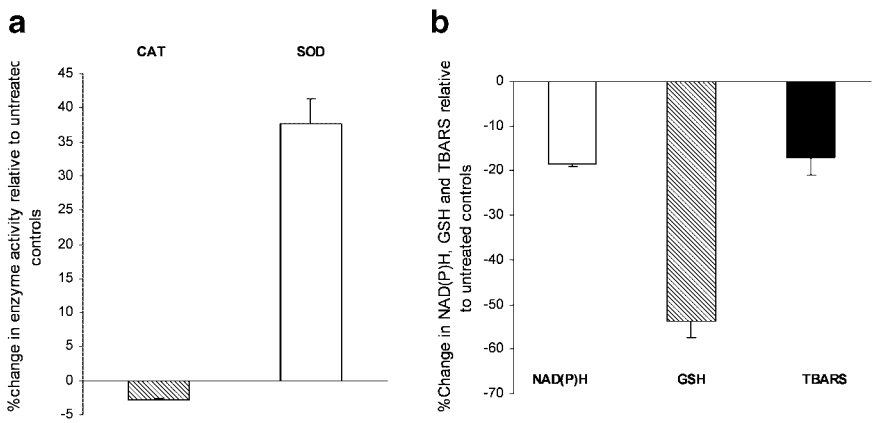

Fig. 5. Fat-loading increases SOD activity and induces a positive redox shift. **a**: Day 7 spheroids from HepG2 cells fat-loaded for 48 h with 0.15 mM oleic acid were assayed for catalase (CAT, shaded bar) and SOD (SOD, open bar) activity by fluorescent and luminescent assays, respectively. Data are expressed as % of fluorescence or luminescence relative to untreated controls corrected for total protein (mg). n = 3, mean ± SD. **b**: Spheroids treated as in ''a'' were assayed for NAD(P)H via lysate absorbance at 340 nm (NAD(P)H, white bar), reduced glutathione (GSH) determined by a fluorescent monochlorobimane assay (shaded bar) and oxidative damage determined using a TBARS assay (TBARS, black bar). Data are expressed as % absorbance/fluorescence relative to untreated controls corrected for total protein (mg). n = 3, mean ± SD.

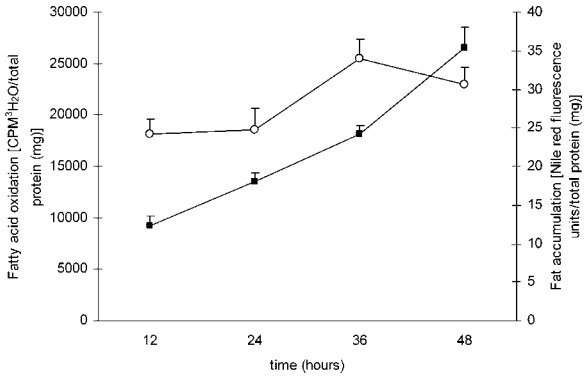

Fig. 6. Fat oxidation and fat accumulation by fat-loaded spheroids. Day 7 spheroids were fat-loaded for 48 h with 0.15 mM oleic acid spiked with ^{3}H-oleic acid. Medium from 12 h time points was used to assess fatty acid oxidation (square) which is expressed as CPM tritiated water per total protein (mg), n = 4, mean ± SD. Cells were also assessed for fat accumulation at these time points by Nile red staining and spectrofluorimetry (open circle). Fat accumulation expressed as Nile red fluorescence units × (10^3) per total protein (mg), n = 3, mean ± SD.

lipogenesis and gluconeogenesis [Kawaguchi et al., 2002; Rutter et al., 2003]. We found that glucose transport was indeed increased by fat-loading (Fig. 7A) and that both lipogenesis and gluconeogenesis were reduced, in fat-loaded spheroids in comparison to non-fat-loaded controls (Fig. 7B,C).

Collectively, these findings suggested a possible increase in the activity of AMPK in steatotic spheroids. To confirm this, HepG2 spheroids were exposed to 0.15 mM oleic acid for 48 h. We observed a marked phasic change in AMPK activity during this time course with a rise in response to fat-loading over 12–36 h followed by a return to control levels at 48 h (Fig. 8), confirming that fat-loading did indeed enhance AMPK activity levels for HepG2 spheroids.

Reduced AMPK Activity Induces Lipotoxicity and Diminishes Steatosis-Dependent Protection Against Pro-Oxidant Induced Cytotoxicity

To investigate further the hypothesis that AMPK activation contributed to the protective effect of fat-loading against TBH-induced oxidative stress, HepG2 cells were transiently transfected with a vector constitutively expressing a c-myc-tagged kinase-dead AMPKα2 catalytic subunit [Mu et al., 2001], encapsulated

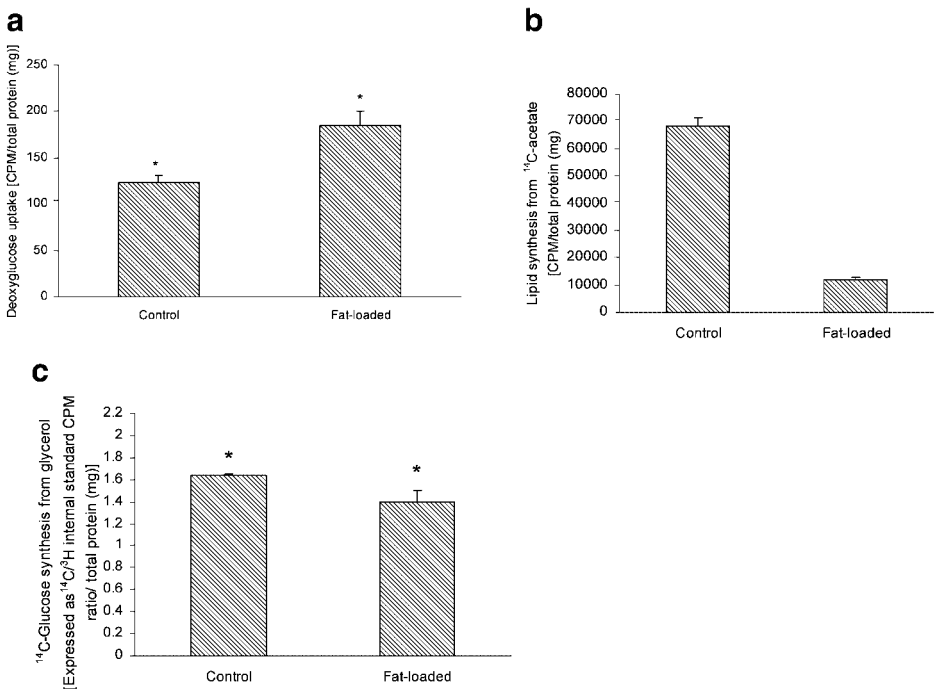

Fig. 7. Fat-loaded spheroids exhibit increased glucose transport, reduced lipogenesis, and reduced gluconeogenesis. Day 7 spheroids were untreated (Control) or fat-loaded with 0.15 mM oleic acid for 48 h (Fat-loaded) and (**a**) incubated with 0.25 μCi/ml 2-deoxy-d-[1-^{3}H] glucose to determine glucose transport or (**b**) pulse labeled for 3 h with ^{14}C-acetate and de novo lipid synthesis determined. Data are expressed as counts per minute (CPM) per mg total protein, n = 3, mean ± SD. **c**: Untreated (Control) or fat-loaded spheroids were also incubated with ^{14}C-glycerol and total ^{14}C-glucose measured relative to a tritiated glucose internal standard. Results are averages of three experiments and expressed as the ratio of ^{14}C/^{3}H counts per minute (CPM) per total protein (mg), n = 3, mean ± SD, (*$P < 0.05$).

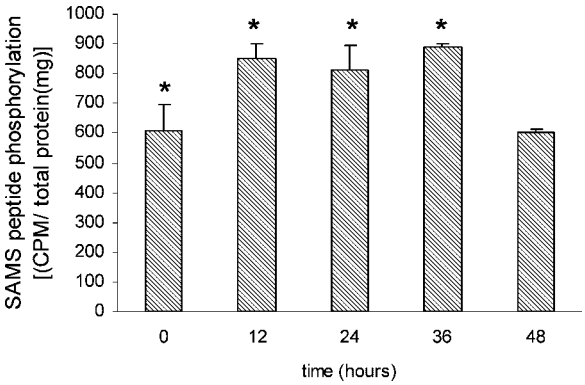

Fig. 8. AMPK activity for HepG2 spheroids. Day 7 HepG2 spheroids were fat-loaded with 0.15 mM oleic acid over 48 h and AMPK activity determined at 12 h intervals. Results are averages of two experiments and expressed as CPM per total protein (mg), n = 3, mean ± SD. (*$P < 0.05$).

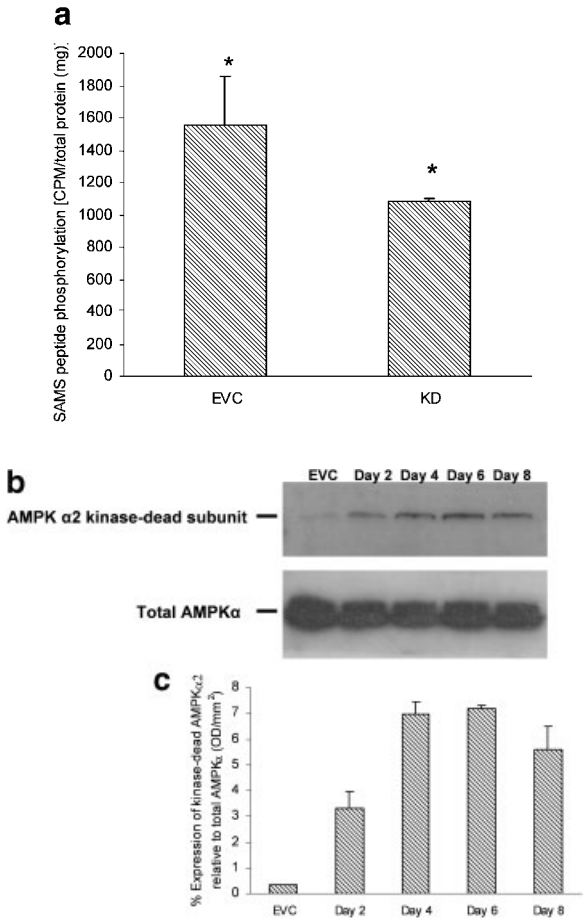

Fig. 9. Expression of c-myc tagged AMPKα2 kinase-dead (KD) subunit by HepG2 transfectants. **a**: AMPK activity for HepG2 spheroids transfected with an empty pcDNA3 vector (EVC) or with pAMPK α2 K45R (KD). Results are averages of three assays, (*$P < 0.05$). **b**: Spheroids from HepG2 cells transfected with an EVC or with pAMPK α2 K45R constitutively expressing a KD AMPK α2 subunit (KD) were assessed over 8 days. Protein from spheroids at 2-day intervals was equally loaded (100 μg per well) onto and separated by SDS–PAGE, blotted and probed with an anti-c-myc antibody. Membranes were stripped and re-probed with an anti-AMPKα antibody. **c:** Bands were detected by ECL and quantified by laser densitometry, and KD levels expressed as a % of total AMPKα, n = 3, mean ± SD.

in alginate and maintained for 7 days in 3-D culture. Spheroids were then fat-loaded for 48 h and treated with the pro-oxidant TBH. Kinase-dead transfectants exhibited a 30% reduction in AMPK activity after 8 days of culture in comparison to empty vector control transfectants (Fig. 9A). Western analysis to verify the level of kinase-dead AMPKα2 protein expression relative to total AMPKα protein levels indicated sustained expression of kinase-dead AMPKα protein from Day 4, reaching a maximum of ~7% by Day 6 of culture (Fig. 9B,C). The kinase-dead (catalytically inactive) α2 subunit inhibits AMPK function by binding to AMPK β and γ subunits, forming functionally inactive heterotrimeric AMPK complexes.

Figure 10A confirmed that for empty-vector control transfectants exposed to TBH for 18 h, as in normal HepG2 spheroids, fat-loading protected cells from TBH-induced cytotoxicity with reduced SYTOX Green fluorescence (columns 1 vs. 2). In these control transfectant cells, the cytotoxicity observed in the presence of fat was 36% of that in non-fat loaded cells ($P < 0.05$).

No significant difference in cytotoxicity was observed for TBH-treated non-fat loaded kinase-dead transfectants in comparison to non-fat loaded empty vector control transfectants (columns 1 vs. 3). However, in kinase-dead transfectants, the protective effect of fat-loading was significantly reduced (columns 3 vs. 4). Cytotoxicity in the presence of fat was 64% of that observed in non-fat loaded cells ($P < 0.05$). Furthermore, fat-loaded kinase-dead transfectants exhibited increased cytotoxicity compared to fat-loaded empty vector controls (columns 2 vs. 4; $P < 0.05$). Thus with decreased AMPK activity, the protective effect of fat-loading was reduced.

Interestingly, TBARS assays demonstrated that fat-loading, in the absence of pro-oxidant challenge, more than doubled the increase in TBA-reactivity in kinase-dead transfectants compared with empty-vector controls—that is, with reduced AMPK activity and in the absence

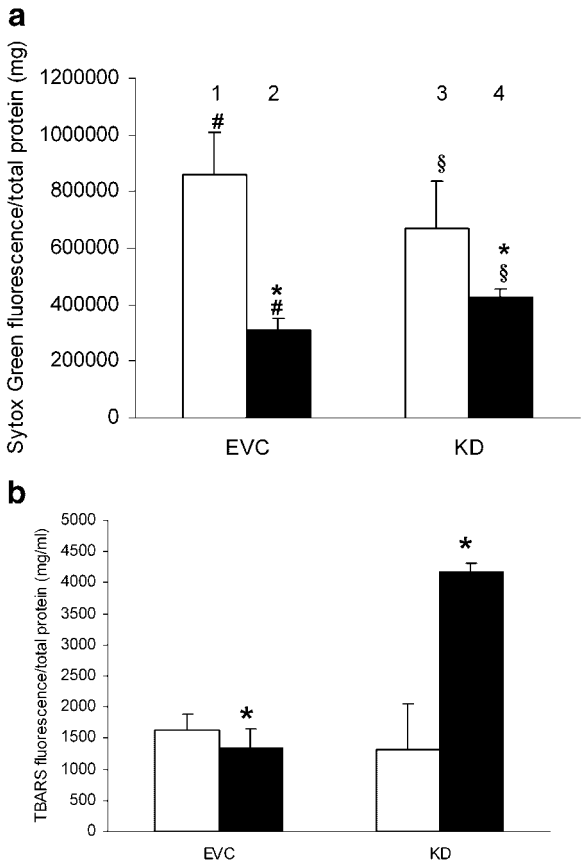

Fig. 10. Reduced AMPK activity increases TBH-induced cytotoxicity for fat-loaded spheroids and induces lipotoxicity. **a**: Day 7 spheroids from HepG2 cells transfected with an empty pcDNA3 vector (EVC) or with pAMPK α2 K45R constitutively expressing a kinase-dead AMPK α2 subunit (KD) were untreated (open bar) or fat-loaded with 0.15 mM oleic acid for 48 h (black bar). Transfectants were then exposed to 0.5 mM TBH for 18 h with SYTOX green and fluorescence quantified. Results are averages of three experiments of n = 3 mean ± SD. Fat-loading significantly decreased TBH-induced SYTOX Green fluorescence for the EVC transfectants ($^{\#}P < 0.05$) and KD transfectants ($^{\S}P < 0.05$). TBH-induced SYTOX Green fluorescence was significantly increased for fat-loaded, KD transfectants in comparison to fat-loaded EVCs ($^{*}P < 0.05$). **b**: EVC and KD transfectants untreated (open bar) or fat-loaded as above (black bar) were assayed for oxidative stress using a TBARS assay. Data are expressed as fluorescence per total protein (mg), n = 3 mean ± SD. Fat-loading significantly increased TBARS fluorescence for KD transfectants in comparison to EVCs ($^{*}P < 0.05$).

of pro-oxidant challenge, lipotoxicity was observed (Fig. 10B). This contrasts with our findings in HepG2 cells, where fat phasically activates AMPK (Fig. 8); in normal fat-loaded spheroids there is protection against lipotoxicity, as well as the resistance to damage by TBH already demonstrated. This protection is also seen in the empty vector control transfectants.

Furthermore, the previously observed steatosis-dependent induction of SOD activity in fat-loaded spheroids was significantly reduced in kinase-dead transfectants. Lucigenin luminescence (inversely proportional to SOD activity) was reduced by 38% in fat-loaded empty vector control cells and 9.8% for fat-loaded kinase-dead transfectants (Fig. 11A). The ability of fat-loading to lower reduced glutathione levels and NAD(P)H (i.e., to induce a positive redox shift) was also significantly impaired for kinase-dead transfectants in comparison to fat-loaded empty vector controls (Fig. 11B,C, respectively). Collectively, these findings strongly suggested that AMPK activation was an important component of the observed fat-induced preconditioning effect observed in our model.

DISCUSSION

In this study, we investigated the susceptibility of steatotic hepatocyte-derived cells to TNFα and the pro-oxidant, TBH.

We established that a 3-D HepG2 culture model exposed to 0.15 mM oleic acid for 48 h induced steatosis in spheroids by Nile red staining and electron microscopy.

It was initially surprising to find that in this model, fat-loading decreased TNFα and TBH-induced cytotoxicity, since it is currently believed that steatosis generates oxidative stress and increases hepatocyte susceptibility to oxidative damage observed in NAFLD [Day, 2002; Sanyal, 2005].

For our model, we observed a substantial decrease in GSH levels, a positive shift in intracellular redox potential and a significant increase in SOD activity for fat-loaded spheroids, agreeing with the hypothesis that steatosis induces a pro-oxidant state. However, this pro-oxidant shift occurred in the absence of oxidative damage—that is, steatosis induced metabolic alterations, sufficient to stimulate oxidative defence mechanisms, not sufficient to cause oxidative damage, and serving to precondition against more severe pro-oxidant challenge.

Our observation that spheroids transiently transfected with a plasmid expressing a kinase-dead AMPKα2, subunit, which induced a significant but partial (30%) downregulation of AMPK activity, exhibited a significant reversal of the fat-induced protective effect, increased

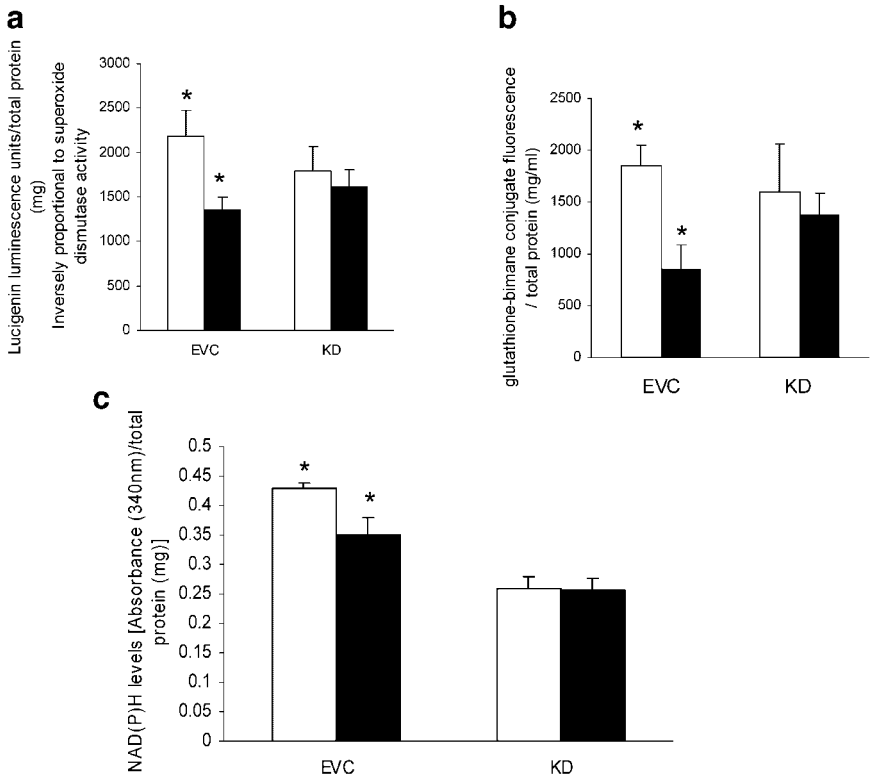

Fig. 11. AMPK KD transfectants fail to exhibit increased SOD activity and a positive redox shift when fat-loaded. **a**: Empty vector controls (EVC) or kinase-dead tranfectants (KD) were untreated (open bar) or fat-loaded with 0.15 mM oleic acid (black bar) for 48 h. SOD activity was determined using a lucigenin luminescence assay based on the ability of SOD to quench superoxide-dependent lucigenin luminescence. Therefore SOD activity is inversely proportional to luminescence. Data are expressed per total protein (mg), $n = 3$ mean $\pm$ SD. **b**: EVC and KD transfectants untreated (open bar) or fat-loaded as above (black bar) were assayed for reduced glutathione (GSH) by bimane-fluorescence or (**c**) NAD(P)H by absorbance at 340 nm. Fluorescence and absorbance data expressed per total protein (mg). $n = 3$, mean $\pm$ SD. Fat-loading significantly decreased lucigenin luminescence, GSH fluorescence, and NAD(P)H absorbance in EVC transfectants for subparts a–c ($^*P < 0.05$) but not in KD transfectants.

lipotoxicity (determined by TBARS) and a failure by fat to induce SOD activity and a positive redox shift, strongly implies that AMPK plays an important role in this preconditioning phenomenon.

These observations are supported by studies which show that 0.15 mM concentrations of fatty acids activate AMPK in hepatocytes, in turn triggering the "glucose sparing" effect—the inhibition by fatty acids of hepatic glucose metabolism and lipogenesis [Kawaguchi et al., 2002]—which we also observed for steatotic spheroids. Therefore, we speculate that fat-loading HepG2 spheroids increases fatty acid oxidation and AMPK activity, in turn down-regulating biosynthetic pathways and simultaneously increasing oxidative metabolism via the glucose sparing effect. An increase in oxidative metabolism would increase ROS production leading to increased demand for GSH and NADPH and thus the observed decline in these metabolite levels upon fat-loading. This effect, not sufficient to induce cell damage, would trigger: (1) increased SOD activity, and (2) increased NADPH production, by enhanced glucose transport and flux through the pentose phosphate pathway, as well as decreased NADPH consumption via lipogenesis, leading to increased glutathione reduction rates. These combined effects would thus decrease cell susceptibility to severe oxidative stress. The observation that AMPK kinase-dead transfectants exhibit far lower (approx 50%) NAD(P)H than controls accords with this hypothesis (Fig. 11C).

AMPK activity can be directly inhibited by long-chain acyl-CoA esters [Taylor et al., 2005], suggesting that fat metabolism may negatively regulate AMPK activity via acyl-CoA ester accumulation in the cell. This could account

for the return to baseline kinase activity after 48 h fat-loading, and explain the differences between our findings and those of Feldstein et al. [2004]. These authors, using fatty acid concentrations three- to sixfold greater than this study, found steatosis to directly induce toxicity via lysosomal destabilization and cathepsin B release in HepG2 cells [Feldstein et al., 2004]. With high concentrations of fatty acids, a rapid accumulation of acyl-CoA esters may result in the early inhibition of AMPK, impairing the adaptive response and thus leading to lipotoxicity.

Although the inhibition of AMPK activity leads to a significant impairment of the fat-induced adaptive response, kinase-dead transfectants only exhibit a partial reversal of the fat-induced protective response upon TBH exposure. This indicates that whilst AMPK is important, it is not the sole contributor to the fat-induced protective response. The role of other potential mediators of this protective response such as specific protein kinase C (PKC) isoforms (e.g., PKCε), known to be activated by unsaturated fatty acids in a variety of cell types including HepG2 cells and hepatocytes [Diaz-Guerra et al., 1991; Sung et al., 2004], and shown to protect against stressors such as ischemia-reperfusion injury [Mackay and Mochly-Rosen, 2001], needs to be clarified.

Overall, we demonstrate that a steatotic phenotype is not in itself sufficient to cause enhanced susceptibility to cytokine or pro-oxidant-induced damage in hepatocyte-derived cells. The possible implications of these findings are that: (a) hepatocytes readily adapt to a steatotic/fat metabolizing phenotype without cellular damage (supported by the fact that only 3% of those with steatosis progress to steatohepatitis), and (b) a perturbation of the mechanisms required for this adaptive process results in direct lipotoxicity and increased susceptibility to oxidative stress.

Interference with the metabolic/energy status of hepatocytes via perturbance of AMPK appears one likely contributor to the multi-hit process underlying the progression of human fatty liver disease.

ACKNOWLEDGMENTS

The authors gratefully acknowledge Dr M.J. Birnbaum (Howard Hughes Medical Institute, Philadelphia, PA) for providing AMPK plasmid and Mr I. Clatworthy of the Royal Free Hospital for the electron microscopy studies.

REFERENCES

Damelin LH, Coward S, Choudhury SF, Chalmers S, Cox IJ, Robertson NJ, Revial G, Miles M, Tootle R, Hodgson HJ, Selden C. 2004. Altered mitochondrial function and cholesterol synthesis influences protein synthesis in extended HepG2 spheroid cultures. Arch Biochem Biophys 434:167–177.

Day CP. 2002. Pathogenesis of steatohepatitis. Best Pract Res Clin Gastroenterol 16:663–678.

Day CP, James OF. 1998. Steatohepatitis: A tale of two "hits"? Gastroenterology 114:842–845.

Diaz-Guerra MJ, Junco M, Bosca L. 1991. Oleic acid promotes changes in the subcellular distribution of protein kinase C in isolated hepatocytes. 266:23568–23576.

Farrell GC, Larter CZ. 2006. Non-alcoholic fatty liver: From steatosis to cirrhosis. Hepatology 43:S99–S112.

Feldstein AE, Werneburg NW, Canbay A, Guicciardi ME, Bronk SF, Rydzewski R, Burgart LJ, Gores GJ. 2004. Free fatty acids promote hepatic lipotoxicity by stimulating TNF-alpha expression via a lysosomal pathway. Hepatology 40:185–194.

Greenspan P, Mayer EP, Fowler SD. 1985. Nile red: A selective fluorescent stain for intracellular lipid droplets. J Cell Biol 100:965–973.

Jones LJ, Singer VL. 2001. Fluorescence microplate-based assay for tumor necrosis factor activity using SYTOX Green stain. Anal Biochem 293:8–15.

Kawaguchi T, Osatomi K, Yamashita H, Kabashima T, Uyeda K. 2002. Mechanism for fatty acid "sparing" effect on glucose-induced transcription: Regulation of carbohydrate-responsive element-binding protein by AMP-activated protein kinase. J Biol Chem 277:3829–3835.

Khalil M, Shariat-Panahi A, Tootle R, Ryder T, McCloskey P, Roberts E, Hodgson H, Selden C. 2001. Human hepatocyte cell lines proliferating as cohesive spheroid colonies in alginate markedly up-regulate both synthetic and detoxificatory liver function. J Hepatol 34:68–77.

Lenaerts I, Braeckman BP, Matthijssens F, Vanfleteren JR. 2002. A high-throughput microtiter plate assay for superoxide dismutase based on lucigenin chemiluminescence. Anal Biochem 311:90–92.

Lieber CS. 2004. CYP2E1: From ASH to NASH. Hepatol Res 28:1–11.

Machado M, Cortez-Pinto H. 2005. Non-alcoholic fatty liver disease and insulin resistance. Eur J Gastroenterol Hepatol 17:823–826.

Mackay K, Mochly-Rosen D. 2001. Arachidonic acid projects neonatal rat cardiac myocytes from ischaemic injury through epsilon protein kinase C. Cardiovasc Res 50:65–74.

McCullough AJ. 2006. Pathophysiology of non-alcoholic steatohepatitis. J Clin Gastroenterol 40:S17–29.

Mu J, Brozinick JT Jr, Valladares O, Bucan M, Birnbaum MJ. 2001. A role for AMP-activated protein kinase in contraction- and hypoxia-regulated glucose transport in skeletal muscle. Mol Cell 7:1085–1094.

Nobili V, Pastore A, Gaeta LM, Tozzi G, Comparcola D, Sartorelli MR, Marcellini M, Bertini E, Piemonte F. 2005. Glutathione metabolism and antioxidant enzymes in

patients affected by nonalcoholic steatohepatitis. Clin Chim Acta 355:105–111.

Rodriguez-Antona C, Donato MT, Boobis A, Edwards RJ, Watts PS, Castell JV, Gomez-Lechon MJ. 2002. Cytochrome P450 expression in human hepatocytes and hepatoma cell lines: Molecular mechanisms that determine lower expression in cultured cells. Xenobiotica 32: 505–520.

Rutter GA, Da SX, Leclerc I. 2003. Roles of 5′-AMP-activated protein kinase (AMPK) in mammalian glucose homoeostasis. Biochem J 375(Pt 1):1–16.

Salt IP, Johnson G, Ashcroft SJ, Hardie DG. 1998. AMP-activated protein kinase is activated by low glucose in cell lines derived from pancreatic beta cells, and may regulate insulin release. Biochem J 335(Pt 3):533–539.

Sanyal AJ. 2005. Mechanisms of Disease: Pathogenesis of non-alcoholic fatty liver disease. Nat Clin Pract Gastroenterol Hepatol 2:46–53.

Scharnagl H, Schinker R, Gierens H, Nauck M, Wieland H, Marz W. 2001. Effect of atorvastatin, simvastatin, and lovastatin on the metabolism of cholesterol and triacylglycerides in HepG2 cells. Biochem Pharmacol 62:1545–1555.

Sebastia J, Cristofol R, Martin M, Rodrigues-Farre E, Sanfeliu C. 2003. Evaluation of fluorescent dyes for measuring intracellular glutathione content in primary cultures of human neurons and neuroblastoma SH-SY5Y. Cytometry 51A(Pt A):16–25.

Shimabukuro M, Zhou YT, Lee Y, Unger RH. 1998. Troglitazone lowers islet fat and restores beta cell function of Zucker diabetic fatty rats. J Biol Chem 273: 3547–3550.

Sung M, Kim I, Park M, Whang Y, Lee M. 2004. Differential effects of dietary fatty acids on the regulation of CYP2E1 and protein kinase C in human hepatoma HepG2 cells. J Med Food 7:197–203.

Taylor EB, Ellingson WJ, Lamb JD, Chesser DG, Winder WW. 2005. Long-chain acyl-CoA esters inhibit phosphorylation of AMP-activated protein kinase at threonine 172 by LKB1/STRAD/MO25 Am J Physiol Endocrinol Metab 288:E1055–61.

Wu M, Lin Z, Wolfbeis OS. 2003. Determination of the activity of catalase using a Europium(III)-tetracycline-derived fluorescent substrate. Anal Biochem 320:129–135.